REPORT

C. D. Storlazzi · E. K. Brown · M. E. Field
K. Rodgers · P. L. Jokiel

A model for wave control on coral breakage and species distribution in the Hawaiian Islands

Abstract The fringing reef off southern Molokai, Hawaii, is currently being studied as part of a multi-disciplinary project led by the US Geological Survey. As part of this study, modeling and field observations were utilized to help understand the physical controls on reef morphology and the distribution of different coral species. A model was developed that calculates wave-induced hydrodynamic forces on corals of a specific form and mechanical strength. From these calculations, the wave conditions under which specific species of corals would either be stable or would break due to the imposed wave-induced forces were determined. By combining this hydrodynamic force-balance model with various wave model output for different oceanographic conditions experienced in the study area, we were able to map the locations where specific coral species should be stable (not subject to frequent breakage) in the study area. The combined model output was then compared with data on coral species distribution and coral cover at 12 sites along Molokai's south shore. Observations and modeling suggest that the transition from one coral species to another may occur when the ratio of the coral colony's mechanical strengths to the applied (wave-induced) forces may be as great as 5:1, and not less than 1:1 when corals would break. This implies that coral colony's mechanical strength and wave-induced forces may be important in defining gross coral community structure over large (orders of 10's of meters) spatial scales.

Communicated by Geological Editor P.K. Swart

C. D. Storlazzi (✉) · M. E. Field
Coastal and Marine Geology Program, US Geological Survey,
Pacific Science Center, 1156 High Street,
Santa Cruz, CA 95064, USA
E-mail: cstorlazzi@usgs.gov
Tel.: +1-831-4274721
Fax: +1-831-4274748

E. K. Brown · K. Rodgers · P. L. Jokiel
Hawaii Institute of Marine Biology,
University of Hawaii at Manoa,
P.O. Box 1346, Kaneohe, Hawaii 96744, USA

Introduction

Computer models are being increasingly used to simulate aspects of coral reefs, including carbonate production (Aigner et al. 1989; Bosence and Waltham 1989) and the geologic development of reef structures over the course of sea-level fluctuations (Bosscher and Schlager 1992). Such simulations help in understanding the various controls on reef structures; however, separating the influence of individual controls remains difficult. Without quantification of the individual controls, computer simulations on reef growth will depend on the use of empirical data on biologic, geologic, and environmental variables (Graus et al. 1984; Scaturo et al. 1989; Bosscher and Schlager 1992). Typically, most simulations combine data from different geological and geographical settings, causing significant problems when trying to understand how a specific biologic, geologic, or oceanographic system interacts to form a specific reef structure.

It has been known for some time that there are strong qualitative correlations between wave energy and coral distribution (Rosen 1975; Geister 1977; Vosburgh 1977b; Dollar 1982; Done 1983; Massel and Done 1993; Rogers 1993; Blanchon and Jones 1997). Grigg (1998) has most recently discussed the interplay between wave energy and reef properties in the Hawaiian Islands, but as in most past studies, wave energy is classified in terms of the loosely divided categories of "low", "medium", or "high" wave energy regimes. Jokiel et al. (2004) show that maximum wave height in Hawaii is negatively correlated with coral cover, diversity, and species richness. There has yet to be, however, a large-scale quantitative investigation of these relationships that compares the motions exerted by waves upon the reef to the distribution of different stony coral species. Our goal

is to better quantify the interplay between wave-induced forces and coral species distribution. This was accomplished by analyzing the wave-induced forces acting on Hawaiian stony coral forms and estimating the magnitudes of mechanical stresses induced by these forces. These calculations were then used to predict failure envelopes for different coral species under varying wave heights, wave periods, and water depth combinations. This hydrodynamic force-balance model was then tested with modeled wave data and spatially-extensive data on coral species distribution off southern Molokai, Hawaii.

Study area

The island of Molokai is located roughly 21°N, 157°W in the north-central Pacific between the islands of Oahu and Maui in the Hawaiian Archipelago (Fig. 1). The island is 62 km long in the east–west direction and on average 13 km wide north–south. A 40-km-long fringing coral reef lies off the south shore of the island in the channels between Molokai, Lanai, and Maui. The actively growing reef pinches out roughly 7 km from the west end of the island and 22 km from the east end.

Most fringing coral reefs can be subdivided into three general parts: the reef flat, the reef crest, and the fore reef. The reef flat off southern Molokai is shallow, generally less than 2 m, and attains a maximum depth of 3 m except in certain locations where 'blue holes' with nearly vertical walls extend to depths of more than 10 m. The reef flat is on average 1 km wide and has a maximum width of more than 1.5 km offshore of the saddle between the two basaltic shield volcanoes that compose the island. Low coral cover (typically < 10%) and shore-normal 'ridge-and-runnel' structures (Blanchon and Jones 1997) extending from the shoreline out to the reef crest characterize the reef flat. The reef crest is well defi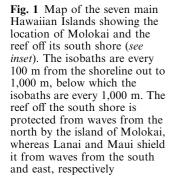ned off south Molokai and is characterized by irregular morphology dominated by robust coral microatolls. The crest is typically 1–2 m deep and is the zone where most deepwater waves break. The fore reef, which extends from the reef crest to depths of approximately 30 m, is the zone of highest coral cover and is generally characterized by shore-normal 'spur-and-groove' structures, large "blue holes", re-entrants, and paleo-stream channels that correspond to onshore drainages.
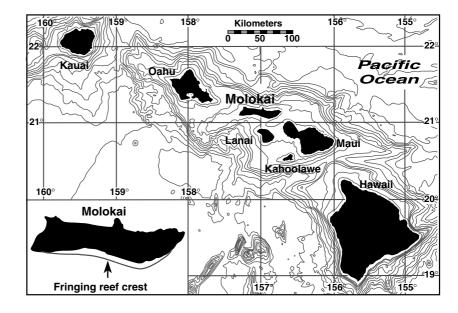
The wave climate off Molokai is dominated by four wave regimes: the North Pacific swell, northeast trade wind waves, southern ocean swell, and Kona storm waves (Moberly and Chaimberlain 1964). North Pacific swell is generated by strong winter (November–March) storms as they track from west to east across the North Pacific and have significant wave heights (H_s) ~3–8 m and peak periods (T_p) ~10–20 s. The northeast trade wind waves occur throughout the year, but are largest from April through November when the trade winds blow the strongest; these waves have H_s ~1–4 m, but have very short periods (T_p ~5–8 s). The southern swell is generated by storms in the southern ocean during the southern hemisphere winter; although the waves are typically small (H_s ~1–2 m), they have very long periods (T_p ~14–25 s). Kona storm waves occur when local fronts or extratropical lows pass through the region and are neither frequent nor consistent in their occurrence. Kona storm waves typically have H_s ~3–5 m and T_p ~8–12 s.

Methods

Coral coverage

Qualitative estimates of percent areal coral coverage were collected using visual estimation techniques patterned after the accuracy assessment scheme for the NOAA habitat mapping efforts in Hawaii, Puerto Rico,

Fig. 1 Map of the seven main Hawaiian Islands showing the location of Molokai and the reef off its south shore (see inset). The isobaths are every 100 m from the shoreline out to 1,000 m, below which the isobaths are every 1,000 m. The reef off the south shore is protected from waves from the north by the island of Molokai, whereas Lanai and Maui shield it from waves from the south and east, respectively

and the US Virgin Islands (Kendall et al. 2001; Coyne et al. 2003). In many situations such visual estimates are more reproducible and more accurate than random-point sampling (Dethier et al. 1993). Two experienced observers estimated percent total coral cover on hard substrata and dominant species coverage as the boat drifted a distance of 30 to 50 m using lookboxes (diameter 0.3 m) from the survey vessel. The repeated estimates by different observers were always in good agreement and were averaged. These estimates were verified by in-situ visual examination during reconnaissance snorkels and scuba dives in February 2000. Observations were logged over a broad area at each of 12 locations spaced ~1.6 km along the 10-m isobath from the west end of the island east to Kaunakakai on the south shore of Molokai from the R.V.*Alyce C.* By making observations along the 10-m isobath, cross-shore variations in species zonation due to such factors as variations in light availability for photosynthesis (Stoddart 1969; Dustan 1982; Falkowski et al. 1990) were reduced. This method made it possible to relate variations in the coral distribution to along-shore variations in the physical environment. The dominant species recorded were the delicate finger coral *Porites compressa*, two similar low energy species; *Montipora capitata* and *Montipora patula*, which display a more compact form than *P. compressa*; *Pocillopora meandrina*, a more robust, moderate energy species; and *Porites lobata*, a high-energy species (Grigg 1983).

Wave modeling

In order to provide accurate wave data for locations along the south shore of Molokai, the US Naval Oceanographic Office's Spectral Wave Prediction System (SWAPS) version 4.0 wave model (WAM) was used. The WAM is an energy-balanced, spectral wave model with variable resolution; this version related surface roughness and drag coefficients to wave formation and had improved response to refraction effects from variable bottom morphology. It defines the spectral energy of wind-generated waves using 25 frequency bands and 24 direction bands. Surface wind forcing for the global and higher resolution local WAM was derived by the US Fleet Numerical Meteorology and Oceanography Center's NORAPS model. A one-degree global WAM drove the finer-resolution WAM model area as boundary input. The model's resolution for the study area was 1.6×1.6 km. The model generated a gridded field of wave height, period, and direction for analysis. Since the WAM product was wind generated, once inside the 10-m isobath, shallow-water interactions were not indicated in the gridded model output. This depth of 10 m, therefore, was the minimum depth for which we could compute our hydrodynamic force model using the spatial WAM data. This was not a problem, however, because this was the isobath along which we collected the coral coverage data. Ultimately, we wished to compare the maximum modeled wave-induced forces encountered along the south shore to the observed distribution of different coral species. In order to do this, a synthetic maximum set of forces that the reef experienced was computed by selecting the wave parameters that would result in the largest near-bed shear stresses for each grid cell in the model domain.

Real-time WAM H_s and T_p output were compared with concurrent observations of H_s and T_p made at two US National Oceanographic and Atmospheric Administration (NOAA) deepwater buoys (#51001 and #51002) and five wave/tide gauges we deployed in 11 m off the south shore of Molokai. The WAM output's H_s and T_p values differed from the field data by less than 10% and verified that the model's estimation of energy loss due to refraction and shoaling worked properly. The H_s and T_p for the shallowest grid cells that were closest to the south shore of Molokai output by the WAM were then used to calculate the dominant wave celerity (C, in m/s), the horizontal wave orbital velocity (u, in m/s), the wave orbital amplitude excursion (A_e, one-half of the orbital diameter, in m), and the radian wave frequency (ω, in 1/s) from Stokes' second- and fourth-order wave theory (e.g., Komar 1998). All of these parameters, except for ω, are dependent on some combination of H_s, T_p, and h (e.g., Komar 1998). These parameters were then used for input into the coral force balance model. In order to best visualize the wave-induced forces on the bed, the peak wave-induced near-bed shear stresses under oscillatory flow, $\hat{\tau}_b$,, which incorporate both H_s and T_p, were calculated:

$$\hat{\tau}_b = \frac{1}{2}\rho_f f_w (A_e \omega)^2 \qquad (1)$$

These $\hat{\tau}_b$ values are in Newtons (N) per m^2. The wave friction factor (f_w), which parameterizes the wave shear stress, was set at 0.3 following the observed attenuation in wave heights over the same species of corals on the reef off Kaneohe, Hawaii, by Lowe et al. (2004).

Hydrodynamic force model for coral species distribution

As first discussed by Chamberlain and Graus (1975), a useful model for analyzing hydraulic controls on coral species distribution can be constructed by considering the effect of water movement against a coral form. Flow of fluid around a coral form causes some of the momentum of the fluid to be transferred to the coral. The hydrodynamic forces (lift, drag, and inertia) generated by this momentum transfer induce stresses on the coral, which will cause the coral to break if the applied load exceeds the mechanical strength of the coral form. These are balanced by the weight and strength of the coral, as shown schematically in Fig. 2. In order to simplify the force and stress calculations, the following assumptions along the lines of Graus et al. (1977) were made:
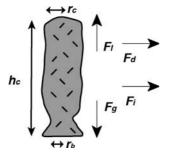
Fig. 2 Diagram of forces on a coral and the parameters used to define a coral's morphology. F_g, F_l, F_d, and F_i are the coral's weight and the wave-induced lift, drag, and inertial forces, respectively. The morphologic parameters include the coral height, h_c, the coral's radius, r_c, and the coral's basal radius, r_b

1. Corals are represented as idealized cylinders. Due to the solitary (*P. compressa* and *P. lobata*) or very densely branched (*M. capitata* and *P. meandrina*) coral forms being investigated, we felt this simplification was valid.
2. Skeletal structure and thus strength are uniform throughout the coral form. Hence the stress will be greatest at the base of the coral where it attaches to the substrate.
3. The position of the center of dynamic pressure and the center of mass for the coral coincide and lie at the midpoint of the coral height.

Weight of the coral is a function of coral colony's morphology and acts to counter the forces of lift and drag, which act to dislodge the coral from the substrate. The weight of a coral (F_g) is purely a function of the coral's relative density and volume:

$$F_g = (\rho_c - \rho_f) g \pi r_c^2 h_c \qquad (2)$$

where the coral skeletal density, $\rho_c = 1{,}450$ kg/m³ (Lough and Barnes 1992), the fluid density, $\rho_f = 1{,}024$ kg/m³ for seawater at 20 °C and salinity of 33.5 psu, and the coral's radius, r_c and height, h_c is a function of the species' colony form (Fig. 2). Representative values for the parameters that define the idealized morphology of the different coral species were estimated from numerous in-situ measurements collected over the course of 22 scuba dives made throughout the study area (Table 1).

As fluid flows over an object, the flow is disturbed as flow lines diverge and the fluid temporarily accelerates over the object; this acceleration over the object causes a lifting force. The lift force (F_l) on a coral was defined as:

$$F_l = \frac{1}{2} \rho_f C_l \bar{u}^2 2 r_c h_c \beta \qquad (3)$$

with the dominant near-bed horizontal wave orbital velocity, u calculated from Stokes' second-order wave theory, the lift coefficient, $C_l = 0.15$ (Hoerner 1965, for a cylindrical shape), and a "hiding" parameter, β that is also a function of the coral species. This parameter

Table 1 Coral morphologies and mechanical strengths used in the model. Mechanical strength data are from Rodgers et al. (2002)

Coral species	h_c (m)	r_c (m)	r_b (m)	σ_{mean} (Mpa)
Montipora capitata	0.20	0.10	0.06	3.5
Porites compressa	0.15	0.02	0.02	5.3
Porites lobata	1.00	0.50	0.45	6.2
Pocillapora meandrina	0.20	0.13	0.07	7.0

accounts for how much of the individual coral is exposed to the flow, or conversely, is not hidden by other corals; β varies from 0–1 (total blocking of flow to no blocking of flow, respectively). Seeing some corals are on the edge of coral spurs or are solitary ($\beta = 1.0$) whereas others are surrounded by other corals ($\beta < 0.5$), we choose the $\beta = 0.9$ value somewhat arbitrarily. Our basis for this selection is that this value lies within the range of numerous field observations and seeing it is most likely that the wave-induced forces would likely have a greater influence on corals near the edge of a group of corals, in that a failure of a coral at the edge of a group would then expose the corals further in the group, decreasing their β. This choice is further supported because the choice of a value of β slightly less than 1.0 would help to take into account some of the high bottom roughness on the length scales of coral spurs (orders of 10's of meters) that cannot be adequately addressed by f_w and the drag coefficient, C_d. Moving water imposes a drag force on any structure projecting into and disrupting the flow. The drag force (F_d) on a coral was defined as:

$$F_d = \frac{1}{2} \rho_f C_d \bar{u}^2 2 r_c h_c \beta \qquad (4)$$

where we set the drag coefficient, $C_d = 0.85$ based on the range of values of 0.7–1.0 determined for corals and rough cylinders by Denny (1988, 1993) and Gerhart et al. (1993). Of note is that laboratory measurements on rough cylinders and real corals indicate that C_l and C_d values are relatively constant across a range of Reynolds numbers (Denny 1988; Gerhart et al. 1993) and thus variable C_l and C_d numbers based on the Reynolds numbers are not needed and likely invalid. Since the passage of a wave causes oscillatory flow, inertial forces are present due to the acceleration and deceleration of the flow field around the coral head as the wave boundary layer grows and decays. The inertial force (F_i) on a coral due to this acceleration is defined as:

$$F_i = \frac{51}{24} \rho_f \pi r_c^2 h_c a \qquad (5)$$

where the local fluid acceleration around a coral head, a, is function of u and T_p. This formulation is based on the solution found by Massel (Eq. 7.77, 1996), but is solved for the more typically observed cylindrical coral shape.

As discussed by Graus et al. (1977), F_i and F_d act above the base of the coral to induce an overturning moment about the neutral axis. The neutral axis passes

through the center of mass and is perpendicular to the flow direction. F_l and F_g do not directly contribute to the overturning moment because they act along the neutral axis. The overturning moment lifts the upstream edge of the coral base and forces down on the downstream edge, causing tension on the upstream edge and compression on the downstream edge. These stresses are superimposed on the stresses induced by the F_g and F_l and reverse with every half T_p of the wave. The resulting overturning moment (sum of applied forces per unit area or stresses) needed to break the coral from the substratum was then solved following Massel's equation 7.85 (1996):

$$\sum \sigma_{applied} = \frac{F_g + F_l}{\pi r_b^2} - \frac{\frac{1}{2}(F_i + F_d)2r_c r_b}{\frac{1}{4}\pi r_b^4} \qquad (6)$$

where the basal coral radius, r_b, is function of the species' colony form.

Corals are primarily composed of aragonite, which has been shown to be very stiff and brittle (Vosburgh 1977a; Tunnicliffe 1979). These studies showed that corals typically bend very little under large forces and fail suddenly with little deformation. The amount of force necessary to cause a coral of a specified strength to fail can be computed in the laboratory (Tunnicliffe 1982; Rodgers et al. 2002). Rodgers et al. (2002) calculated coral tensional and compressional strengths in the lab from prism-shaped pieces of the coral species *Porites compressa*, *Pocillopora meandrina*, *Montipora capitata* and *Porites lobata*; these strengths are listed in Table 1. Because corals undergo both tensional and compressional forces under oscillatory wave motion, the mean value of the two mechanical strengths or resistive forces per unit area ($\overline{\sigma}_{resistive}$) was used to compare to the wave-induced forces for analysis.

Since the parameter u is a function of both H_s and T_p, which vary not only along-shore but also in the cross-shore direction as the water depth varies, we computed the wave-induced stresses on corals a range of depths over which these corals have been observed in the field. For each coral species, the force balance was computed for a range in wave conditions for $H_s = 1$–7 m and $T_p = 4$–28 s in 0.5-m and 2-s steps, respectively. Water depths were also varied, from $h = 5$–30 m at 5-m intervals. In order to better understand the relative balance of these forces, a factor of safety, *Fs*, which is the ratio of the resistive forces per unit area (mechanical strength) to the applied stresses defined in Eq. (6), was calculated:

$$Fs = \frac{\overline{\sigma}_{resistive}}{\sum \sigma_{applied}} \qquad (7)$$

Thus, a *Fs* = 50 means that the coral's strength is 50 times greater than the applied "breaking" forces, while a *Fs* < 1 implies that the coral will fail (break) as the applied forces are greater than the coral's strength. These calculations can then be validated by comparing maps of actual coral species distribution along the 10-m isobath to maps of different species' calculated *Fs* values along the 10-m isobath. For example, if a specific coral species was observed at a location where the predicted Fs > 1, the model would appear valid; conversely, if the calculated Fs < 1 for a certain location and the specific species and was not observed, the model would also appear to support the model's effectiveness.
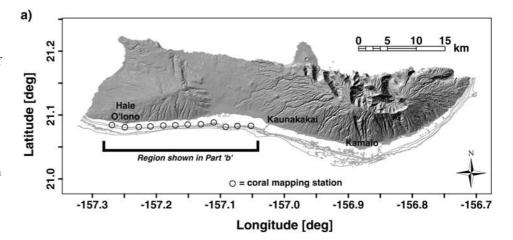
Results

Coral distribution

Observations of coral coverage along the 10-m isobath were conducted at 12 locations stretching > 20 km from the west end of the island east to Kaunakakai on the south shore of Molokai (Fig. 3a). Total coral coverage is extremely high, typically greater than 90% of hard surfaces except near the west end of the island, where the total coral cover drops sharply (Fig. 3b). *Porites compressa* dominates most of the central portion of the reef, composing more than 70% of the coral observed; its abundance also decreases towards the island's west end. *Porites lobata*, a more robust species, typically composes only 6% of the coral covered substrate at 10 m. Within 8 km of the west end of Molokai, it reaches a maximum abundance of 60% of the total coral observed before it decreases to 50% at the western-most mapping station. *Montipora* spp. (consisting of *M. captiata* and *M. patula*) generally composes approximately 17% of the hard substrate, increases to 60% at 9.5 km from the island's west end and essentially disappears at the west end. *Pocillopora meandrina* is generally uncommon (∼3%) along most of the reef, except in the western-most stations where it composes between 20 and 50% of total coral coverage noted. Overall, coral coverage is highest and relative diversity is lowest along south-central portion of the island, which is protected from the largest waves, whereas coral coverage decreases, but relative species diversity increases, towards the west end of the island where the wave energy is very high.

Wave modeling

The SWAPS WAM was run for the four main wave regimes for the Hawaiian Islands and a commonly observed combination of a North Pacific swell and trade wind waves (Table 2). The wave events modeled corresponded to the largest waves observed for each regime over the previous 15 years for which there was high enough quality boundary conditions data to run the WAM. We chose to use the largest events observed over the previous 15 years seeing that this length of time approaches the recovery time for the coral species addressed here (Dollar 1982; Grigg 1983) and that corals and their resulting reefs generally develop under the

Fig. 3 Location of coral mapping sites and the resulting data on coral coverage. **a** Map of the island of Molokai showing the relative position of the coral mapping sites made along the 10-m isobath along with the names of areas discussed in the text. **b** Plot of the along-shore variation in total coral cover ($\pm\sigma$) and species distribution along the south shore of Molokai. Overall, total coral cover is high towards the lower-energy south-central portion of Molokai, whereas total coral cover is low towards the southwest corner of the island where wave energy is the highest. It is clear from the figure that the *Porites compressa* and *Montipora* spp. coverage goes to zero, and that robust *Porites compressa* and *Pocillopora meandrina* make up most of what is left of the coral cover on the wave-impacted west end
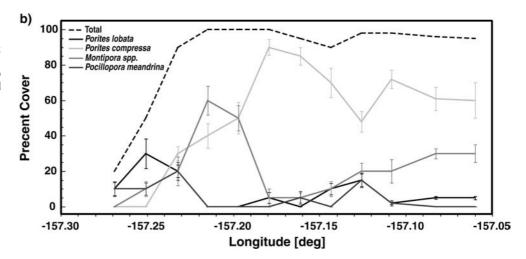

Table 2 SWAPS WAM modeling conditions. Data are from NOAA-NDBC buoys #51001 and #51002. Note: θ_{wave} is the direction from true north the waves are coming from

Wave regime	Date (mm/dd/year)	H_s (m)	T_p (s)	θ_{wave} (deg)	U_{wind} (m/s)
North Pacific swell	01/28/1998	8.4	20	320	6.1
Kona storm waves	08/16/1998	2.8	9	170	7.2
Southern Ocean swell	06/08/2000	2.5	20	180	6.2
Trade wind waves	06/23/1998	3.2	8	50	13.8
Trade wind waves and	11/30/1998	4.6	8 (trade wind)	50 (trade wind)	12.5
North Pacific swell			16 (N Pacific)	350 (N Pacific)	12.5

conditions typically observed over the time necessary for their recovery (Graus 1984; Rogers 1993). The WAM North Pacific swell run displayed a strong shadowing effect by the island of Molokai along its southern coast. The north, east, and west sides of the island were exposed to the brunt of this large swell, which could generate near-bed wave orbital velocities (u) greater than 1.75 m/s along most of Molokai's shoreline. The area off the south shore, concurrent with the large fringing reef, is a shadow zone with modeled u less than 0.5 m/s. Along most of the fringing reef, u was less than 0.2 m/s in 10 m of water. At both the east and west ends of the island where the reef narrows, u rapidly increases five-fold to more than 1.0 m/s.

The Kona storm waves, which were modeled to observe how the south shore of Molokai would be impacted by an unrefracted swell, did not generate high near-bed wave orbital velocities ($u = 0.19$ m/s) anywhere along the island, likely due to their relatively short period. The southern ocean swell, on the other hand, produced intermediate u values (~ 0.5 m/s) along almost the entire length of Molokai's fringing reef and have been observed to transport high quantities of fine-grained terrestrial sediment on the fore reef and the reef flat. The modeled trade wind waves appear to primarily impact the east and southeast coast of the island. Due to their short period and intermediate height, these waves produce rather low u values, on the order of 0.3 m/s. In combination with a

typical North Pacific swell, however, the model suggests that much higher orbital velocities impact the east and southeast shore of Molokai, on the order of 0.8–0.9 m/s in the area where the reef starts to pinch out.

The synthetic maximum modeled wave conditions are dominated by the large (8 + m), long-period (22 s) North Pacific winter waves along the entire north shore and both the east and west ends of Molokai (Fig. 4). Due to refraction, some of this energy wraps around the west end of the island, generating very high orbital velocities upon the south shore up to a few kilometers from the west end of the island. The rest of the south shore of Molokai is in the shadow of Molokai from these large North Pacific waves and exhibit moderately low (<0.5 N/m^2) peak bed stresses. Whereas the majority of the south shore is in this wave shadow, the coastline between the southernmost point of the island at Kamalo and the east end of the island is directly exposed to trade wind waves. This exposure caused the modeled horizontal wave-orbital velocities and peak bed shear stresses to be slightly ($\sim$0.25 N/m^2) higher than to the west of Kamalo, which is in the lee of the point. The trade wind waves' short period are reflected in the greater disparity between the peak bed shear stresses at 5 and 10 m east of Kamalo than to the west of Kamalo where the coastline is not directly impacted by these waves. Along the deeper isobaths (15 and 20 m) near the east end of the island, the peak bed shear stresses are more similar to those observed to the west of Kamalo.
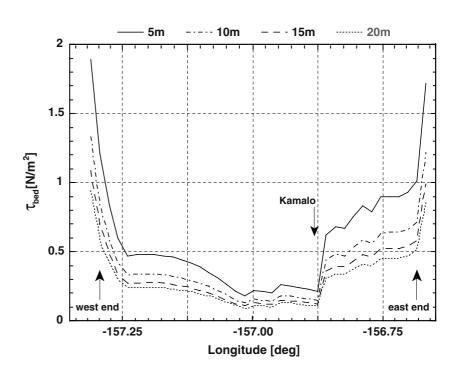
Hydrodynamic force modeling

The coral species' modeled failure regimes for a range of wave heights, wave periods, and water depths are shown in Figs. 5 and 6. These failure regimes or "envelopes" are defined as the combination of wave heights and period above which the specific coral will break for a specified water depth. The larger failure envelopes for *Porites compressa* and *Montipora capitata* (Fig. 5) versus those at similar depths for *Pocillopora meandrina* and *Porites lobata* (Fig. 6) reflect the combination of coral strength and growth form. For example, *Porites compressa*'s mechanical strength is more than 50% greater than *Montipora capitata*'s (Table 1); however, the more delicate thin "finger" form of *Porites compressa* makes it more susceptible to wave-induced forces versus the weaker but more stout growth form of *Montipora capitata*. In all of these cases, wave-induced forces and thus the extent of failure envelopes decrease with increasing water depth and decreasing wave height and period. Additional model runs varying the drag coefficient (C_d) by 50% to test its sensitivity produced failure envelopes slightly smaller or larger (differences ≤ 0.5 m and 2 s increase in wave height and period, respectively), but did not change the relative distribution between the species based on their mechanical strengths.

Interestingly, the vertical distribution of these same corals in the Hawaiian Islands we have observed in the field, and elsewhere described by Dollar (1982) and Grigg (1983), can be explained by these modeled failure envelopes in Figs. 5 and 6. The shallower ($h \sim 5$ m) portions of south and west-facing Hawaiian reefs are typically dominated by *Pocillopora meandrina* and *Porites lobata*, which were calculated to be stable ($Fs > 1$) under "typical" wave conditions ($H_s < 3$ m, $T_p < 15$ s) encountered over the course of a year. Under these same "typical" conditions, the computations show that both *Porites compressa* and *Montipora capitata* at these same depths would break ($Fs < 1$) under the applied wave
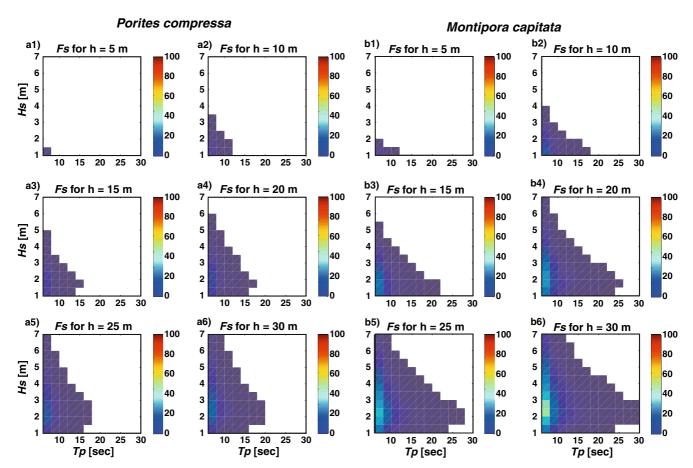

Fig. 4 Variation in maximum modeled wave-induced peak bed shear stresses with depth along the south shore of Molokai. Most of the high stresses associated with the large, long-period North Pacific winter waves typically drop off dramatically >3 km from the ends of the island. The higher modeled stresses east of Kamalo are caused by the open exposure of this section of the reef to trade wind waves, which directly impact this section of shoreline through the channel between Molokai and Maui. Most of the rest of the south shore is in the lee of Lanai from southern ocean swell

Fig. 5 Factors of safety and failure envelopes for the two of the four corals investigated. **a** *Porites compressa*. **b** *Montipora capitata*. Each subplot (#1–6) displays the ratio of the wave-induced forces to the coral's mechanical strength for a different water depth between $h = 5$ m and $h = 30$ m. *White regions* denote the wave conditions (failure envelope) defined by significant wave height (H_s) and peak wave period (T_p) under which the specified coral species would break when the wave-induced forces exceed the coral's mechanical strength. The *colored regions* are the sets of wave conditions under which the corals are stable. Both species have larger failure envelopes (factor of safety, Fs < 1) at shallower depths than at deeper depths due to the exponential decay in wave energy with water depth. Note that even though *M. capitata* has a lower mechanical strength than *P. compressa*, that *M. capitata*'s failure envelopes (*white regions*) are smaller for a given water depth due to its more compact shape

stresses. Conversely, at depths of 15 m where *Porites compressa* and *Montipora capitata* are commonly observed to dominate the available substrate, the modeling shows that under these same "typical" conditions both of these species have Fs > 10.

Discussion

Spatial distribution of coral species' Fs off southern Molokai

By applying the hydrodynamic force-balance model to the spatial wave model's synthetic maximum wave con-

ditions data set, it was possible to map the spatial distribution of each coral species' Fs around the island of Molokai, as shown in Fig. 7. More robust species such as *Pocillopora meandrina* and *Porites lobata* have higher Fs values and thus are stable over much larger areas than the more delicate *Porites compressa* and *Montipora capitata*. One factor that is not taken into account by these Fs distributions is competition between different coral species. In areas where both are stable and well suited for growth, one species will tend to out-compete the other by faster growth (Glynn and Wellington 1983), aggression (Lang 1973; Genin et al. 1994), or more successful recruitment (Smith 1992). In Hawaii, observations by Maragos (1972), and Grigg and Maragos (1974) indicate that as physical disturbance or wave exposure decreases, certain species such as *Porites compressa* and *Montipora capitata* out-compete other species for space and dominate the available habitat. These studies suggest that a hierarchy exists in terms of competition and growth rate between species from most successful to least successful: *Porites compressa* > *Montipora capitata* > *Pocillopora meandrina* > *Porites lobata*. This hierarchy was used as the basis for inter-species competition that would delineate which species would dominate the available substrate under a given set of wave conditions and not exceed the Fs for any of the species.

In continuing with the assumption made here that wave forces are a primary control on coral species'
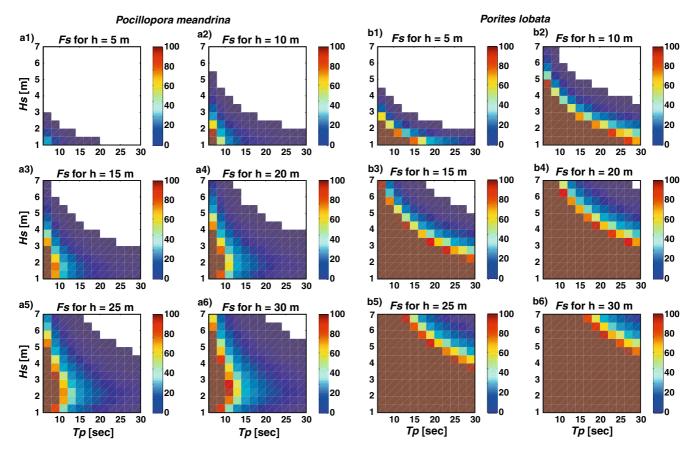
Fig. 6 Factors of safety and failure envelopes for the two of the four corals investigated. **a** *Pocillopora meandrina*. **b** *Porites lobata*. Each subplot (#1–6) display the ratio of the wave-induced forces to the coral's mechanical strength for a different water depth between $h = 5$ m and $h = 30$ m. *White regions* denote the wave conditions (failure envelope) defined by significant wave height (H_s) and peak wave period (T_p) under which the specified coral species would break when the wave-induced forces exceed the coral's mechanical strength. The *colored regions* are the sets of wave conditions under which the corals are stable. Both species have larger failure envelopes (factor of safety, $Fs < 1$) at shallower depths than at deeper depths due to the exponential decay in wave energy with water depth. Note that these two corals have much smaller failure envelopes (*white regions*) for a given depth than those in Fig. 5 due to their higher mechanical strengths and sturdy growth forms

general spatial distribution at a given depth, a number of simulations were run in which it was assumed that the dominant coral species would be replaced by another when a specified *Fs* was exceeded. To investigate the interaction between inter-species competition and wave control on coral species distribution, first the entire grid space was initially set to be populated by *Porites compressa* since it tends to out-compete all of the other species when the location is suitable hydrodynamically. Some arbitrary *Fs* limit was then chosen. For example, when the arbitrary *Fs* limit was set to be 5, when *Porites compressa's Fs* < 5 at some grid cell, the grid cell was then set to *Montipora capitata*, and when *Montipora capitata's Fs* < 5 at the same grid cell, it was replaced by *Pocillopora meandrina* and so on. A series of *Fs* cut-off

values were then run and compared with the observed distribution of coral species off the south shore of Molokai (Fig. 8).

The *Fs* values that best correlate with the observed coral species distribution lie somewhere between 3–5 (Fig. 8). This, by itself, would imply that the dominant but most fragile coral species would give way to the next most dominant (and more robust) species when its strength is less than three to five times the applied breaking forces. This suggests that physical factors other than wave-induced breaking of the corals might be more important in defining general coral species distribution. Such factors may include the variation in thickness of the hydromechanical boundary layers representing differences in requirements for plankton and nutrient supply (Chamberlain and Graus 1975; Shashar et al. 1996), structural weakening due to dissolution and excess nutrients (Hallock and Schlager 1986), and abrasion by suspended sediment or previously broken pieces of coral (Harmelin-Vivien and Laboute 1986). This brings light to a very interesting point that is not incorporated in the model. If a piece of coral, for example a "finger" of *Porites compressa*, was weakened due to biological, chemical, or mechanical erosion it could break and detach from the substrate under lower imposed forces or a higher *Fs* (i.e., *Fs* = 2) than needed to break a full-strength piece of coral at a *Fs* = 1. This detached piece of coral rubble could then be suspended by wave-induced water motions and impact other live, full-strength corals

Fig. 7 Results from a model run displaying the input maximum wave conditions and the resulting distribution of factor of safety (*Fs*) values for different species in the study area. **a** Map of modeled significant wave height, *H*$_s$ from the WAM. **b** Map of modeled peak wave period, *T*$_p$ from the WAM. **c** Modeled *Fs* distribution for *Porites compressa*. **d** Modeled *Fs* distribution for *Montipora capitata*. **e** Modeled *Fs* distribution for *Pocillopora meandrina*. **f** Modeled *Fs* distribution for *Porites lobata*. Note the much larger regions with high *Fs* values for the more robust *P. meandrina* and *P. lobata* species versus the more delicate *P. compressa* and *M. capitata*. The regions with high *Fs* values for *P. compressa* and *M. capitata* off south-central Molokai and southwestern Maui correspond to the two largest active fringing reefs in the main eight Hawaiian Islands
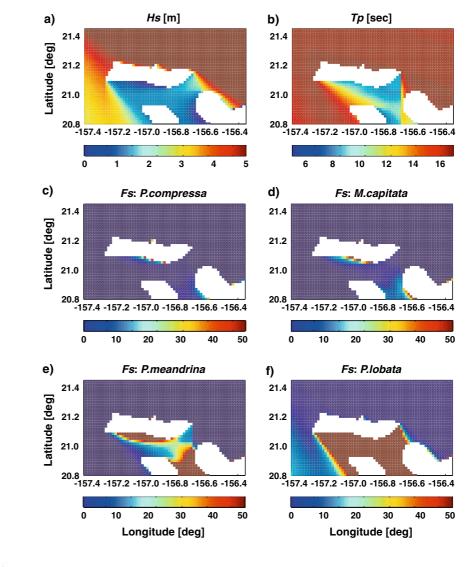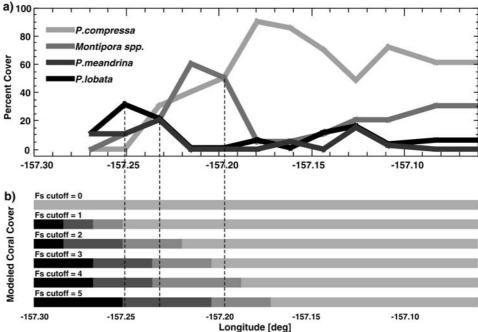

Fig. 8 Comparison of different factor of safety (*Fs*) values for delineating the distribution of dominant coral species off the south shore of Molokai versus the observed coral species distribution. **a** Plot of the alongshore variation in total coral cover and species distribution along the south shore of Molokai. **b** Coral species distributions predicted by the model for a number of different *Fs* values. The best correlation between the model and the observations of the transitions from one species to another occurs with a *Fs* cutoff between 3 and 5. This suggests that the transitions from one species to another may be related to corals weakened by erosion failing at *Fs* > 1 rather than the full-strength corals modeled here predicted to fail at *Fs* < 1

nearby. Combined with the wave-induced forces on the coral form incorporated in the model presented here, these impact forces could exceed the force levels necessary to break the surrounding full-strength corals at a Fs = 1. To examine this "weakest link" concept further, we investigated the amount of reduction in mechanical strength necessary to reproduce the observed distribution.

Using a series of simulations, it was found that a reduction in coral mechanical strength of roughly 20–30% could very well explain the coral species distribution observed. The calculations of mechanical strength by Rogers et al. (2002) were based on solid prisms of coral, thus a reduction of 20–30% seems possible given the high variability in strength and bioerosion.

Model applications

Since this model is based strictly on the balance between the wave-induced forces acting on the coral and the corals' strengths and morphologies rather than empirical data, it can be used to provide information for a number of different problems. For example, this model could be used to predict the impact of severe but infrequent storms or hurricanes. Corals and their resulting reefs develop under the conditions typically observed over the time necessary for their recovery (Graus 1984; Rogers 1993). Because the frequency of extreme events is lower than recovery rates of the corals described here (Dollar 1982; Grigg 1983), sections of coral reefs are commonly damaged by the impact or close passage of an extreme storm or hurricane. This model can be used to predict the locations where these coral species investigated might be broken, based on water depth and the observed wave conditions. Conversely, the breakage of particular corals at a given depth can be used to infer minimum wave forces and the probable range of wave heights and periods that produced the resulting coral failure. Such calculations would also make it possible to better constrain paleo-environmental analyses from ancient corals, such as from drill cores or stratigraphic sections by better defining the hydrodynamic limits that set accommodation space for specific coral species on a given reef. It will be necessary, however, to better constrain the model through more measurements of the variability in the corals' mechanical strengths due to factors such as bioerosion, more accurate modeling of the coral forms, and better field testing of the model prior to any paleo-environmental application.

Conclusions

A hydrodynamic force-balance model was developed to calculate wave-induced forces on stony corals and predict the hydraulic conditions under which four Hawaiian corals would fail and break. The model was tested against a data set on coral species distribution along the south shore of Molokai, Hawaii. Results from the modeling and this test suggest that wave-induced forces are a primary control on coral species distribution over large (orders of 10's of meters) spatial scales and that the transition in general abundance from one species to another along the reef is likely influenced by the corals' strengths and wave conditions typically observed over the course of a few decades.

It is clear that number of other physical factors, such as light availability for photosynthesis and water salinity or temperature, act as primary controls on coral species distribution in areas where these factors are at or near the suitable limit for a specific coral species' growth. Around most of the Main Hawaiian Islands, however, where none of these other physical parameters are at or near their limits, it is clear that wave-induced forces are a primary control on large-scale coral reef development and general species distribution. This is evident in that substantial active reef development has only occurred in areas protected from large waves. At the same time, however, this does not imply that many, if not all, of these corals can be found elsewhere in the islands but rather that they are only found in isolated areas protected from the high wave-induced forces, typically from the North Pacific winter swell. Thus, the wave-induced forces appear to delineate the spatial extent for each of these species over large (orders of 10's of meters) areas, and only when the wave-induced forces are low enough to permit the coral's development can other secondary factors such as overtopping and shading become important in delineating the dominant species along a given stretch of reef.

Despite the model's complexity, it only provides but a small but important piece to our understanding of the natural controls on coral reef ecosystems. Future modifications to be added include functions for light intensity to limit the depth at which specified coral species will grow and a group of equations to model the interaction of coral growth and sediment to better constrain spur-and-groove and ridge-and-runnel development. Furthermore, the model needs to be tested in other locations to better constrain if the transitions from one species to another typically occur at Fs values of 3–5 as observed off south Molokai, or if they are due to other factors such as the underlying bedrock morphology. Locations suitable for such tests are abundant and include the well-developed reef in Kailua Bay on windward Oahu, the reef between Olowalu and Maalaea in south-central Maui, and the atolls and pinnacles of the northwest Hawaiian Islands. It should be noted that this model, although applicable to other coral genera such as *Acropora*, provided the corals' material strengths and morphologies are known, should not be applied without first constraining the Fs transitions with detailed data on coral species distribution and wave parameters.

Overall, the model appears to help define coral species distribution along the Molokai fringing reef, based solely on the region's general wave climate and the corals' strength and morphologies; these results further

support the long-standing ideas that waves are a dominant control on coral species zonation.

References

Aigner T, Doyle M, Lawrence D, Epting M, van Vilet A (1989) Quantitative modeling of carbonate platforms: some examples. In: Crevello PD, Wilson JL, Sarg JF, Read JF (eds) Controls on carbonate platform and basin development. Spec Publ Soc Econ Paleontol Mineral 44:27–37

Blanchon P, Jones B (1997) Hurricane control on shelf-edge-reef architecture around Grand Cayman. Sedimentology 44:479–506

Bosscher H, Schlager W (1992) Computer simulation of reef growth. Sedimentology 39:503–512

Bosence D, Waltham D (1989) Computer modeling the internal architecture of carbonate platforms. Geology 18:26–30

Chamberlain JA, Graus RR (1975) Water flow and hydromechanical adaptations of branched reef corals. Bull Mar Sci 25:112–125

Coyne MS, Battista TA, Anderson M, Waddell J, Smith W, Jokiel P, Kendell MS, Monaco ME (2003) Benthic habitats of the Main Hawaiian Islands. National Oceanic and Atmospheric Administration, National Ocean Service, Biogeography Program, Silver Springs

Denny MW (1988) Biology and mechanics of the wave-swept environment. Princeton University Press, Princeton, NJ

Denny MW (1993) Extreme drag forces and the survival of wind- and water-swept organisms. J Experiment Biol 194:97–115

Dethier MN, Graham ES, Cohen S, Tear LM. (1993) Visual versus random-point percent cover estimations: 'objective' is not always better. Mar Ecol Prog Ser 96:93–100

Dollar SJ (1982) Wave stress and coral community structure in Hawai'i. Coral Reefs 1:71–81

Done TJ (1983) Coral zonation: it's nature and significance. Perspectives on coral reefs. Australian Institute of Marine Research, pp 69–106

Dustan P (1982) Depth-dependant photoadaptation by zooxanthellae of the reef coral *Monastera annularis*. Mar Biol 68:253–264

Falkowski PG, Jokiel PL, Kinzie RA III (1990) Irradiance and corals. In Dubinsky Z (ed) Ecosystems of the world #25: coral reefs. Elsevier Science, Amsterdam, pp 89–108

Gerhart PW, Gross RJ, Hochstein JI (1993) Fundamentals of fluid mechanics. Addison-Wesley, Menlo Park, CA

Geister J (1977) The influence of wave exposure on the ecological zonation of Caribbean coral reefs. Proceedings of the 3rd International Coral Reef Symposium 1:23–29

Genin A, Karp L, Miroz A (1994) Effects of flow on competitive superiority in scleractinian corals. Limnol Oceanogr 39(4):913–924

Glynn PW, Wellington GM (1983) Corals and coral reefs of the Galapagos Islands. University of California

Graus RR, Chamberlain JA, Boker AM (1977) Structural modification of corals in relation to waves and currents. In: Frost SH, Weiss MP, Saunders JB (eds) Reefs and related carbonates-ecology and sedimentology. Am Assoc Petrol Geol Studies Geol 4:135–153

Graus RR, Macintyre IG, Herchenroder BE (1984) Computer simulation of the reef zonation at Discovery Bay, Jamaica: hurricane disruption and long-term physical oceanographic controls. Coral Reefs 3:59–68

Grigg RW (1983) Community structure, succession, and development of coral reefs in Hawaii. Mar Ecol Progress Ser 11:1–14

Grigg RW (1998) Holocene coral reef accretion in Hawaii: a function of wave exposure and sea level history. Coral Reefs 17:263–272

Grigg RW, Maragos JE (1974) Recolonization of hermatypic corals on submerged lava flows in Hawaii. Ecology 55:387–395

Hallock P, Schlager W (1986) Nutrient excess and the demise of coral reefs and carbonate platforms. Palaios 1:389–398

Harmelin-Vivien M, Laboute P (1986) Catastrophic impact of hurricanes on atoll outer reef slopes in the Tuamotu (French Polynesia). Coral Reefs 5:55–62

Hoerner SF (1965) Fluid-dynamic drag practical information on aerodynamic drag and hydrodynamic resistance. Hoerner Dynamics Drag Co, Bricktown, New York

Jokiel PL, Brown EK, Friedlander A, Rodgers K, Smith WR (2004) Hawaii coral reef assessment and monitoring program: spatial patterns and temporal dynamics in reef coral communities. Pacific Science (in press)

Kendall MS, Kruer CR, Buja KR, Christensen JD, Finkbeiner M, Monaco ME (2001) Methods used to map the benthic habitats of Puerto Rico and the US Virgin Islands. National Oceanic and Atmospheric Administration, National Ocean Service, Biogeography Program, Silver Springs

Komar PD (1998) Beach processes and sedimentation. Prentice Hall, New Jersey

Lang J (1973) Interspecific aggression by scleractinian coral 2: why the race is not always to the swift. Bull Mar Sci 23:260–279

Lough JM, Barnes DL (1992) Comparison of skeletal density variations in *Porites* from the Central Barrier Reef. J Experiment Mar Ecol 155:1–25

Lowe RJ, Falter JL, Bendet MD, Pawlak G, Monismith SG, Koseff JR, Atkinson MJ (2004) Wave transformation and circulation on a barrier reef at Kaneohe bay, Oahu, Hawaii. Eos Trans Am Geophys Union 84(52):OS22J-008

Maragos JE 32(1972) A study of the ecology of Hawaiian reef corals. PhD Thesis, University of Hawaii, Honolulu

Massel SR (1996) Ocean surface waves: their physics and prediction. Advanced series on ocean engineering, vol 11. World Scientific Publishing, New Jersey

Massel SR, Done TJ (1993) Effects of cyclone waves on massive coral assemblages on the Great Barrier Reef: Meteorology, hydrodynamics, and demography. Coral Reefs 12:153–166

Moberly RM, Chaimberlain T (1964) Hawaiian beach systems. University of Hawaii

Rodgers K, Newston C, Cox E (2002) Effects of mechanical fracturing and experimental trampling on Hawaiian corals. Environ Manage 31(3):377–384

Rogers CS (1993) Hurricanes and coral reefs: the intermediate disturbance hypothesis revisited. Coral Reefs 12:127–138

Rosen BR (1975) The distribution of coral reefs. Report Underwater Assoc 1:2–16

Scaturo DM, Strobel JS, Kendall CG, Wendte JC, Biswas G, Bezdek J, Cannon R (1989) Judy Creek: a case study for two-dimensional sediment deposition simulation. In: Crevello PD, Wilson JL, Sarg JF, Read JF (eds) Controls on carbonate platform and basin development. Spec Publ Soc Econ Paleontol Mineral 44:63–76

Shashar N, Kinane S, Jokiel PL, Patterson MR (1996) Hydromechanical boundary layers over a coral reef. J Experiment Mar Biol Ecol 199:17–28

Smith SR (1992) Patterns of coral recruitment and post-settlement mortality on Bermuda's Reefs: comparison to Caribbean and Pacific Reefs. Am Zool 32:663–673

Stoddart DR (1969) Ecology and morphology of recent coral reefs. Biol Rev 44:433–498

Tunnicliffe V (1979) The role of boring sponges in coral fracture. In: Levi C, Boury-Ensault N (eds) Biologie des spongiares. CNRS International no 291:309–315

Tunnicliffe V (1982) The effects of wave-induced flow on a reef coral. J Experiment Mar Biol Ecol 64:1–10

Vosburgh F (1977a) Mechanics of the reef coral *Acropora reticulata*. PhD Thesis, Duke University

Vosburgh F (1977b) The response to drag of the reef coral *Acropora reticulata*. Proceedings of the Third International Coral Reef Symposium, Miami, Florida 2:477–482